

**The Possible Generation of Friction Melts at the Lunar Crater, Buys-Ballot.** Peter H. Schultz, Carolyn H. van der Bogert, Carlé M. Pieters; Geological Sciences, Brown Univ., Providence, RI 02912-1846 (Peter\_Schultz@brown.edu)

**Introduction.** Impact melt is generally interpreted as a product of waste heat created by shock pressures exceeding 500-600 kbars (1, 2). There is increasing evidence, however, that high strain rates also induce sufficient shear heating to contribute significant internal energy during the formation (3, 4) and modification (5, 6) stages of crater formation. This process is particularly relevant for oblique impacts where peak pressures are low but strain rates are high. Here we assess several predicted consequences of this process that can be tested in the lunar cratering record.

**Oblique Impact Process.** As impact angles decrease (referenced to the horizontal), peak shock pressures also decrease, as demonstrated by the reduced crater size and depth (7, 8). For a 10° impact angle, a 15 km/s collision would result in a peak pressure of less than 200 kb, well below minimal levels necessary for melting. Although melting and vaporization does occur through the jetting process, the high velocities of those products exceed lunar escape velocities. Laboratory experiments performed at the NASA Ames Vertical Gun Range (AVGR), however, indicate that oblique impacts also create enhanced target heating through frictional shear with significantly lower downrange velocities (3).

At laboratory scales, the duration of impactor/target contact is only a few microseconds. For a 10 km-diameter impactor striking at 10°, contact time exceeds 10 seconds. During this time, the impactor fails and continues to penetrate. Although the upper portion may decouple and ricochet downrange, the target below the impactor is driven downrange by both momentum coupling and asymmetric shock at high strain rates within the crater (9). In experiments at the AVGR, the surface downrange from the crater is plated by impactor-contaminated melts. This process may account for the contrast in impactor contamination levels at the two Clearwater Lake craters where the West Clearwater melts contain little trace of the impactor but East Clearwater melts contain 5-8% (10).

Consequently, there are three predictions for melt generation and dispersal from an oblique impact. First, floor and downrange rim melts should be produced, even at very low peak pressures. Second, the impactor component should be greater than more vertical impacts since a high strain rate is created by the difference between impactor-driven flow and weakly shocked material below. Hence, impact melt produced by iron-enriched impactors (e.g., H chondrites) should appear mafic, even in a non-mafic target. Third, impactor decapitation downrange and the retained downrange momentum should result in a greater impactor signature in the melt downrange. Although AVGR hypervelocity experiments, however, also suggest that relatively well-preserved impactor materials can be preserved inside the crater (in contrast with common wisdom).

**Lunar Observations.** Buys-Ballot (BB) crater is located deep in the farside highlands (22°N, 175°E), well removed from mare deposits and dark-haloed craters, indicative of ancient buried basalts (11, 12, 13). It exhibits the distinctive signatures of a very low-angle impact: elongate pear-shaped plan (90 km x 60 km), crater widening transverse to the inferred trajectory,

and central peak ridge (8). Based on crater shape, the impact angle was probably about 10°, which would require an impactor about 10 km in diameter to produce a crater of this size. The impact occurred at the edge of a larger crater situated on the inner ring of a large degraded two-ringed basin, Freundlich/Sharanov. As a result of both trajectory and topography, impactor failure during penetration extended the crater downrange, similar to laboratory experiments and certain craters elsewhere.

Prior to Clementine, the only images of BB crater were medium-resolution Lunar Orbiter photographs that, nevertheless, clearly revealed its oblique trajectory, interior melt, and downrange deposits. Clementine data provide higher resolution views but with higher sun angles that clearly reveal dark crater deposits, both inside and downrange. The downrange deposits include both a diffuse component that mantles pre-existing topography and a ponded component that embays and fills topographic lows. These materials appear to connect with the downrange rim. In addition, a higher albedo flow lobe fills the downrange crater extension, and a narrow bench encircles the downrange wall. The bench is not a product of slumping but represents a previously higher level of highly fluid, now-drained material.

Five-color Clementine reflectance spectra were calibrated and photometrically corrected as described in (12). Color composite images clearly reveal the principal character of materials within and around BB. Clastic material associated with the crater ejecta, wall, and central peaks indicate varying degrees of fresh anorthositic highland materials (Fig. 1a). The largest central peak exhibits characteristics of crystalline anorthosite: lack of a 1 μm absorption and slight downturn towards longer wavelengths. The other peaks and ejecta exhibit spectra indicative of either shocked anorthositic breccias and/or soils that do not exhibit the downturn towards longer wavelengths (Fig. 1). The smooth crater floor materials inside (Fig. 2, dark floor) display a somewhat more mafic spectral signature, although the overall reflectivity is significantly higher than typical mare. A fresh crater on this unit exposed material with a prominent high-Ca pyroxene (similar to a gabbro or basalt). The lighter downrange interior lobe also appears more mafic than the interior crater debris (Fig. 1). The downrange exterior pooled deposit (pond, Fig. 2) exhibits a darker, slightly more mafic signature than the interior materials.

**Discussion.** The mafic spectral signatures for interior smooth materials and downrange deposits (diffuse and ponded) might be interpreted as impact-triggered volcanism or impact-exposed mare materials. It is unlikely that they resulted from either. First, it would be highly unusual for an oblique impact to create the requisite deep conduits or pathways for magma due to the shallow level of disruption. No other large impact of comparable age in the region has caused such effects. Second, the anorthositic peaks, crater rubble, and ejecta confirm an impact into a predominantly anorthositic highland target, consistent with observations. And third, the interrelationships among the interior bench encircling the downrange crater

LUNAR FRICTION MELTS: P. H. Schultz *et al.*

interior, the downrange interior lobe, and exterior diffuse deposits and ponded units indicate an emplacement origin contemporary with crater formation.

How are the different compositional units created and dispersed by the impact process? Because of the trajectory for Buys-Ballot, these deposits are actually consistent with expectations. First, it is suggested that the darker spectral signature for the ponded units (MO and MI, Fig. 2) has two plausible origins. The darkening may indicate the effects of high strain rate friction processes (14) and/or there has been significant mixing between impactor (contributing the necessary iron, e.g., a chondrite) and target during friction-generated melting during a low-angle impact. Second, the downrange (MO) melt appears to be darker than the interior melt (MI) indicating either a compositional or textural difference. This difference may be consistent with a greater impactor component resulting from materials closer to the impactor/target interface dispersed downrange as observed in laboratory impact experiments. Third, the melts exhibit less textured surfaces and evidence for low viscosity (interior downrange bench). A lower viscosity melt should be expected for high temperature, Fe-enriched friction melts (6). These more clast-free melts in BB contrast with the rubble-entrained floor melts of other fresh impact craters and would allow lower cooling rates and crystallization as indicated by the abundant ferrous clinopyroxene exposed by a fresh crater. And fourth, a survey

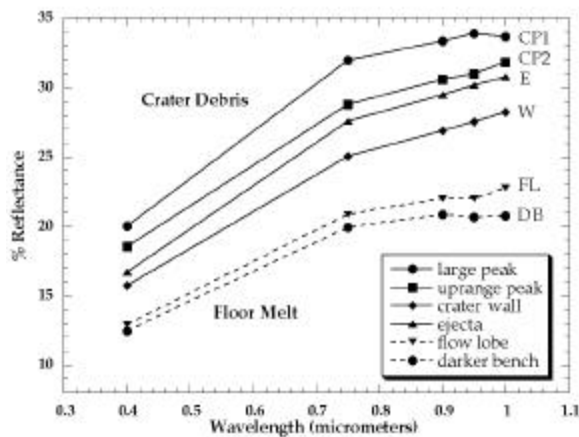


Figure 1. Clementine 5-color spectral data for Buys-Ballot crater materials. The largest member peak of the central ridge exhibits an anorthositic spectrum with crater debris (other peaks, CP, wall, W, and ejecta, E) exhibiting either more highly shocked anorthosites or mixtures. The interior "flow lobe" (IF) corresponds to a steep-sided flow located in the downrange crater extension. The "darker bench" (DB) represents a darker portion of a narrow bench that encircles the downrange interior and appears to be a high-level mark.

of melt deposits associated with other oblique impacts (e.g., King) in the highlands reveal a very similar pattern including a distinct pyroxene spectral band and mafic-appearing dark deposits downrange. The location and age of King (< 0.5 by) precludes a mare source for these materials.

**Conclusions and Implications.** The oblique impact creating Buys-Ballot provides a unique opportunity to assess the possible generation of friction melts (and perhaps impactor contamination). Combined with insights from hypervelocity laboratory experiments, the diversity and distribution of melt types found around certain impact craters might be better understood.

**References.** 1) Engelhardt, W.V. and Stöffler, D. (1968), In *Shock Metamorphism of Natural Materials*, pp. 159-168, Baltimore: Mono Book Corp.; 2) O'Keefe, J.D. and Ahrens, T.J. (1977), *Proc. Lunar Planet. Sci. Conf. 8th*, 3357-3374; 3) Schultz, P.H. (1996), *JGR*, 101, 21,117-21,136; 4) Schultz, P.H. (1996), *GSA Abstracts*, A284; 5) Spray, J.G. (1995), *Geology*, 23, 1119-1122; 6) Spray, J.G. (1993), *JGR*, 98, 8053-8068; 7) Gault, D.E. and Wedekind, T. (1978), *Proc. Lunar Planet. Sci. Conf. 9th*, 3843-3875; 8) Schultz, P.H. and Anderson, R.A. (1996), *GSA Sp. Paper 302*, 397-417; 9) Schultz, P.H. and Gault, D.E. (1990), *GSA Sp. Paper 247*, 239-261; 10) Schultz, P.H. and Gault, D.E. (1990), *Meteoritics*, 26, 392-393; 11) Schultz, P.H. and Spudis, P. (1979), *Proc. Lunar Planet. Sci. Conf. 10th*, 2889; 12) Hawke, B.R. and Bell, J.F. (1981), *Proc. Lunar Planet. Sci. 12th*, 665-678; 13) Antonenko, I. *et al.* (1997), *Lunar Planet. Sci. XXVIII*, 47-48; 14) van der Bogert, C.H., *et al.* (1997), this volume; 15) Pieters, C.M. *et al.* (1997), *GRL*, 24, 1903-1906.

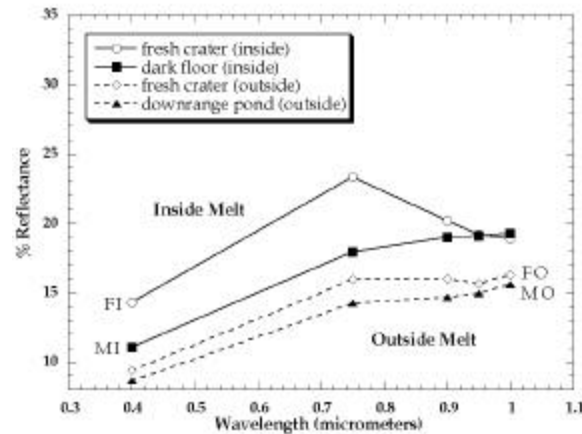


Figure 2. Clementine 5-color spectral data for melts units inside and outside Buys-Ballot. Mature units outside (MO) and inside (MI) exhibit a mafic spectral signature although the downrange pond outside appears to have a lower reflectivity (higher Fe). Freshly exposed materials, however, inside the crater (FI) exhibits a distinct pyroxene band that is only marginally identified outside (FO).